AJEMA GLOBAL RESEARCH NETWORK

AMERICAN Journal of Engineering, Mechanics and Architecture
Volume 3, Issue 7, 2025 ISSN (E): 2993-2637

Examination of the Interaction Between Flow Field and Fatigue Resistance of Gas Turbine Blade using Various Materials

Mahmood A. Mohammed
Department of Mechanical Techniques, Technical Institute Kirkuk, Northern Technical University, Iraq

Abstract: Gas turbines are an important component of power plants. They operate at very high temperatures in combination with rotating at very high speeds, which required the blades to be made up of materials with high resistance. The purpose of the study is to investigate the relationship of the airflow field and the fatigue resistance of a gas turbine blade, where special emphasis will be placed on the effect of blade material. The flow and the stresses put on the blade are simulated by utilizing numerical modeling techniques such as computational fluid dynamics (CFD) and finite element analysis (FEA). The structural performance of blades produced from three distinct materials was investigated: Inconel 718, Ti-6Al-4V, and SiC/SiC CMC. The results revealed that the material has an important influence in the blade's reaction to cyclic loads, with Inconel 718 having the maximum fatigue resistance, with a safety factor of 4.73, compared to 1.18 for Ti-6Al-4V and 0.285 for the SiC/SiC composite. The minimum fatigue life rose by 1159% when Ti-6Al-4V was used instead of Inconel 718, but fell by 98.3% when the ceramic material was used.

Keywords: Turbine, Fatigue, CFD, FEA, life, damage.

Introduction

Gas turbines are key parts of current thermal power systems, changing heat from burning fuel into mechanical energy. Turbine blades are most at risk from mechanical and heat stress since they touch hot, fast-moving gasses [1]. This contact makes the flow uneven, leading to pressure and temperature differences around the blade [2]. These differences lead to repeated strains, which can cause gradual damage, or fatigue [3]. How well a blade resists fatigue affects how long it lasts [4]. Constant heat and mechanical stress from the flow can cause tiny cracks that grow over time, leading to major failure [5,6]. This behavior gets harder to predict because of the blade's material, since each material has different physical and mechanical traits like tensile strength, Young's modulus, heat conductivity, and thermal expansion. These things affect fatigue .[6]

This study looks at how airflow around a gas turbine blade affects its fatigue resistance, comparing how blades made of different materials perform. We will use computer models like CFD to study the flow and FEA to study the resulting structural stresses. We will also study the link between stress and material damage to suggest the best materials for fatigue resistance, which will enhance turbine reliability and life.

Many studies have examined how flow affects turbine blade fatigue resistance, focusing on the mechanical and heat traits of the materials used. Some notable studies include the following.

Zhang et al. made a machine learning model to guess the fatigue life of gas turbine blades using data from finite element analysis.. The study examined GH4169 and TC4 materials and found that material selection had a substantial effect on stress distribution patterns and fatigue fracture start sites [7]. **Sun, D. et al**. conducted an experimental and computational investigation to estimate the fatigue life of aviation engine blades, accounting for the interplay of creep and fatigue under complicated heat flow. The study showed how mimicking real-world multi-field settings can increase modeling accuracy [8]. **Zalapa Garibay et al**. investigated the influence of fatigue-related corrosion on steam turbine blades, and their findings indicated that moist flow accelerates the loss of surface mechanical characteristics, leading to blade failure [9].

Li, M. et al. used a model that included high- and low-cycle fatigue stresses (HCF-LCF) to investigate the lifetime of wind turbine blades. The study concluded that composite materials behave differently depending on the distribution of dynamic stresses caused by flow [10]. **Shah, I., et al**. conducted a comprehensive comparative research of the influence of length, thickness, and material type on the fatigue life of horizontal turbine blades using numerical modeling and lab measurements. It was discovered that the created material has an important role in preventing flow-induced vibrations [11]. **Gonabadi, H. et al**. provided a technique for calculating the fatigue life of marine turbine blades composed of composite materials, and the findings revealed that glass and carbon fibers behave differently under the impact of tidal flow [12].

Patel and Nair conducted comparative research utilizing finite element analysis of two composite materials, glass fiber and carbon fiber, used in the construction of turbine blades, and determined that the material had a direct impact on the blade's stress and fatigue response [13]. **Dhimole et al.** conducted an advanced study on turbine blades built of ceramic composites (CMC), investigating their behavior under thermal and mechanical stresses and demonstrating the superiority of these materials in terms of long-term fatigue and heat resistance [14]. **Kim et al.** investigated the link between the vibrational characteristics of compressor blades and their fatigue resistance, and found that the geometric form of the material, as well as the type of the flow, determines the incidence of frequency stresses that accelerate blade failure [15]. **Sanchez et al**. provided a computational and experimental investigation on fatigue fracture detection in hydro turbine blades, highlighting the value of numerical modeling in finding early crack zones based on turbulent flow model [16].

A. P. Fraas et al. studied the possibility of operating water-cooled gas turbines with a high gas inlet temperature of about $1370C^{o}$, such that the cooling passages are lined with an alloy of chromium, nickel and iron to avoid the occurrence of serious problems [17]**. K. Sagae et al.** also studied the possibility of achieving an efficiency exceeding 60% of a thermal plant at $1700C^{o}$ turbine inlet temperature [18]. **Xing-dan Zhu et al.** studied numerical simulations to gain further insights into the effects of cooling holes with different hole shapes: circular hole, convergent hole, diffuser hole, and cylindrical hole. Using computational fluid dynamics [19].

These investigations, taken together, show that the flow field and the qualities of the produced materials have a complicated impact on turbine blade fatigue resistance. They also underline the significance of integrating numerical and experimental research to have a thorough knowledge of the load and stress distributions. However, there is still a need for a comprehensive comparative analysis that incorporates the impacts of flow and material type into a unified numerical model, which this work aims to address. Despite substantial breakthroughs in understanding the flow dynamics surrounding gas turbine blades and the development of numerical modeling tools for mechanical stress analysis, the majority of prior research have tackled the flow field and fatigue resistance independently or in constrained contexts based on a single material or constant operating circumstances. Furthermore, little study has considered the effect of the blade material within an integrated modeling framework that connects flow and consequent stresses. As a result, a significant research gap exists in understanding the connection between the non-uniform flow field and wear resistance when different materials are utilized to make gas turbine blades.

This is a design difficulty that directly affects the efficiency and operational life of thermal systems.

The purpose of this study is to look at the relationship between the properties of the airflow field around a gas turbine blade and the blade's behavior under fatigue loads caused by this flow, as well as to compare the structural performance and fatigue resistance of various blade materials. This will be accomplished by creating an integrated numerical model that combines computational fluid dynamics (CFD) analysis to simulate flow and finite element analysis (FEA) to investigate the reaction of various materials to repeated stresses, allowing for the determination of the best material in terms of fatigue resistance under actual operating circumstances. In this research, we will use numerical modeling CFD and FEA using Ansys 16.1 software, where the flow field will be studied using CFX software, while the fatigue study will be done using Static structure software, and the results of the pressure field will be taken from CFX software and coupling will be done with Static structure software using one way coupling fluid solid interaction (FSI).

In this project we will use 3 materials and compare them with respect to the relationship betwen flow field and fatigue resistance. These materials are Inconel 718, Titanium alloy i-6AI-4V, and Ceramic Matrix Composite SIC/SIC (CMC). In this research, we have a first-stage gas turbine blade from a 200MW plant. The turbine consists of four stages. We decoded the first-stage blade and drew it using Solidworks using reverse engineering techniques. The blade contains several cooling passages that cool the blade internally to prevent temperatures from exceeding a critical value.

Materials and Methods

In this work, the internal and external flows around the blades will be modeled to obtain the pressure and temperature distribution inside and on the blade surface, respectively. Then, by Finite Element Analysis (FEA), the mechanical fatigue in the blade will be studied with the force and temperature distributions obtained from the CFD study so that the fatigue tolerance of the blade may be studied under three loads in three different materials, and the best type may be selected. The types of materials being studied for the blades are Inconel 718, Titanium alloy i-6AI-4V, and Ceramic Matrix Composite SIC/SIC (CMC). It has a low weight, superior stress resistance, and performs well at high temperatures. It is utilized in applications that need a balance of strength and weight. Ceramic Matrix Composite (SIC/SIC) (CMC) is a ceramic material utilized in contemporary turbine blades where temperatures surpass those of metal alloys. It possesses excellent heat resistance, low weight, and corrosion resistance; however, it is fairly fragile [2,3,5,24].

The **Table 1** and **Table 2** illustrates each mixture's physical qualities, as well as its chemical makeup [24.8].

Table 1 physical properties of materials used

Physical properties	**Inconel 718**	**Ti-6Al-4V**	**SiC/SiC CMC**
density) kg/m³(	8190	4430	2900
Young's modulus) GPa(	200	110	380
Poisson’s Ratio	0.29	0.33	0.17
tensile strength) MPa(	1240	950	300
Fatigue threshold at 10^7 cycles) MPa(	540	510	600
Thermal expansion coefficient) µm/m. K(	13	8.6	4.5
Thermal conductivity) W/m. K(	11.4	6.7	25

Table 2 chemical composition of materials used

element	Inconel 718 (%)	Ti-6Al-4V (%)	SiC/SiC CMC (%)
Ni	50.0–55.0		
Cr	17.0–21.0		
Fe	17.0–Balance	≤0.40	
Nb+Ta	4.75–5.50		
Mo	2.80–3.30		
Ti	0.65–1.15	Balance	
Al	0.20–0.80	5.5–6.75	
Co	≤1.0		
C	≤0.08	≤0.08	
Mn	≤0.35		
Si	≤0.35		
P	≤0.015		
S	≤0.015		
V		3.5–4.5	
O		≤0.20	
N		≤0.05	
H		≤0.015	
SiC Fiber			45–55
SiC Matrix			35–45
Other Binders			5–10

Geometry creation

Due to our inability to know the diminutions of the study blade and its lack of availability within the plant, it was necessary to use reverse engineering technology in order to know the design and dimensions of the model studied in order to complete the modeling process. This part of the research aims to achieve a successful turbine blade engineering that achieves increased gas turbine efficiency and thus a longer lifespan. The research sample was chosen and the gas turbine blade in the Gander thermal power plant was adopted to study all the effects on a model of reality to achieve the true benefit of this research. The cleaning process is particularly important for metal alloys because it gives leak-proof surfaces and increases the life of the alloy. The blade selected in this research was scanned using a 3D laser scanning device.

The process of 3D scanning is divided into several steps: The first step is to identify the object to be scanned and determine the appropriate position for conducting the scan (fixed position - rotating disk), the second step is to perform the scanning process of the part to be scanned, and the third step is processing, where processing refers to the efforts to “clean” and repair the scanning data, which often contains Scanning unwanted content or areas that need more details is done within this stage, and the final step within the scan is to export a three-dimensional mesh model that includes the entire shape with the smallest details. It is exported in several formats, including (STL, OBJ), and then the shape is ready to be modeled as shown in **Figure** 1.

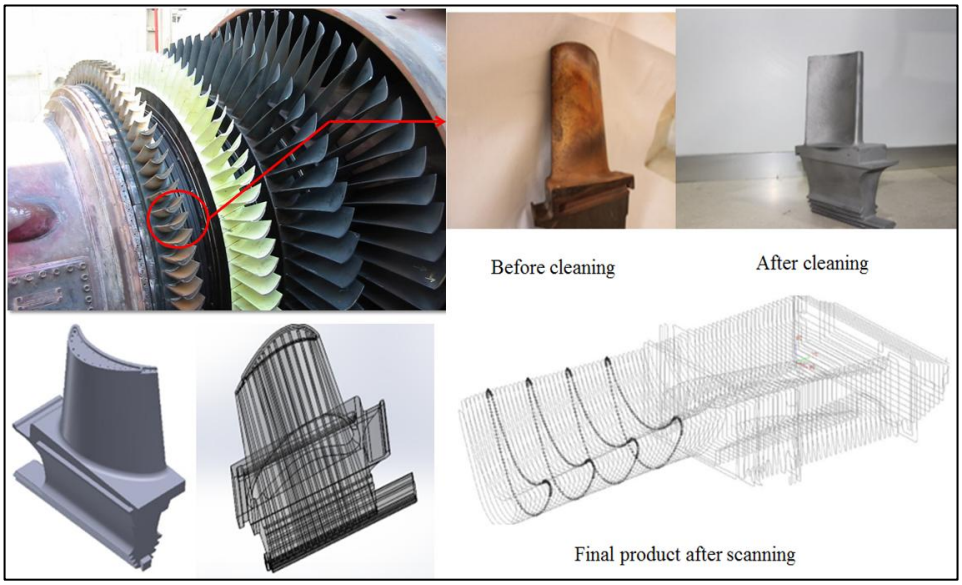

Figure 1 steps to construct blade geometry

In this research, a one-way coupling FSI will be conducted to study the mutual effect between the air flow field across the blade and fatigue endurance of blade for three deferent materials. the study was conduct numerically using Ansys CFX and Static Structure software. Air is considered a compressible fluid whose density changes according to the equation of state for an ideal gas $\rho = \frac{P}{RT}$, where R is the specific gas constant and its value is given to air as $R = 287 \frac{J}{kg.K}$ [16]. The heat capacity of air is calculated as a function of temperature within the CFX software.

Table 3 show these properties

Table 3 Physical properties of air

air	property
$1.7894x10^{-5}$	viscosity μ(Kg/ m.s)
0.0242	λ(W/ m.K) conductivity
Ideal gas	ρ(Kg/ m^3) density
Depend on temperature	C_{pw} (J/ Kg.K) Specific heat

Mathematical model

The physical model consists of the governing equations, which for the flow field are the equation of continuity, momentum, and energy. These equations were written with respect to a coordinate axis that rotate with the blade according to the following relationships [21]:

Continuity equation: $\frac{\partial \rho}{\partial t} + \vec{\nabla}.(\rho \vec{V}_{c/A}) = 0$

Momentum equation: $\rho(\frac{\partial \vec{V}_{c/A}}{\partial t} + (\vec{V}_{c/A}\vec{\nabla})\vec{V}_{c/A} + a_{rel}) = -\vec{\nabla}P + \mu\nabla^2\vec{V}_{C/A} + \vec{F}_b$

Where ρ represents the density of the fluid, $\vec{V}_{c/A}$ represents the relative velocity of the fluid with respect to the moving reference frame (MRF), P represents the pressure and μ dynamic viscosity, whereas $\vec{F}_b$ represents the volumetric forces affecting the fluid element. a_{rel} is the relative acceleration and is given by equation [23]:

$$a_{rel} = \underbrace{2\vec{\Omega}\times\vec{V}_{C/A}}_{1} + \underbrace{\vec{\Omega}\times(\vec{\Omega}\times\vec{V}_{C/A})}_{2} + \underbrace{(a_A + \frac{d\vec{\Omega}}{dt}\times\vec{V}_{C/A})}_{3}$$

Where Ω represents the rotational angular velocity of the coordinate axes.

The first term is the Coriolis acceleration, the second term represents the acceleration resulting from the centrifugal force resulting from rotational motion or centrifugal acceleration, The third term represents the absolute acceleration of the system of moving coordinate axes, as its first term represents the linear acceleration of the moving reference frame relative to the coordinate of fixed axes (absolute acceleration of the moving reference frame) and the second term represents the absolute rotational acceleration of MRF resulting from the rotational movement of this system . The previous equation is a vector equation that has three components on each of the x, y, and z coordinate axes [17].

Energy equation: $\frac{\partial(\rho e_r)}{\partial t} + \vec{\nabla}(\rho\vec{V}_{c/A}h_{or}) = \vec{\nabla}(K\vec{\nabla}T) + \vec{\nabla}(\tau_r\vec{V}_{c/A}) + \vec{F}_b.\vec{V}_{c/A} + \dot{Q}$

The relative internal energy e_r is calculated from the relationship [18]:

$$e_r = h - P/\rho + 1/2(V_{C/A}{}^2 - V_A{}^2)$$

Then the total relative stagnation enthalpy is: $h_{or} = e_r + P/\rho$. τ is the relative shear stress, and $\dot{Q}$ expresses the heat generated within the system due to the presence of an internal source of heat [22].

When calculating the flow field, the value of the pressure resulting from the flow field will be applied to the outer surface of the blade and its inner surface, where there are cooling paths as boundary conditions, in order to study the mechanical effect resulting from the flow field. The resulting temperature distribution within the entire blade will also be taken into account, to take the stresses resulting from heat into account. The governing equation for the mechanical model is [19,20]:

$$\begin{bmatrix}\sigma_x\\ \sigma_y\\ \sigma_z\\ \tau_{yz}\\ \tau_{xz}\\ \tau_{xy}\end{bmatrix} = \frac{E}{(1+\nu)(1-2\nu)}\begin{bmatrix}1-\nu & \nu & \nu & 0 & 0 & 0\\ \nu & 1-\nu & \nu & 0 & 0 & 0\\ \nu & \nu & 1-\nu & 0 & 0 & 0\\ 0 & 0 & 0 & 1-2\nu & 0 & 0\\ 0 & 0 & 0 & 0 & 1-2\nu & 0\\ 0 & 0 & 0 & 0 & 0 & 1-2\nu\end{bmatrix}\begin{bmatrix}\varepsilon_x\\ \varepsilon_y\\ \varepsilon_z\\ \gamma_{yz}\\ \gamma_{xz}\\ \gamma_{xy}\end{bmatrix} - \frac{E}{(1-2\nu)}\begin{bmatrix}\alpha\Delta T\\ \alpha\Delta T\\ \alpha\Delta T\\ 0\\ 0\\ 0\end{bmatrix}$$

etc., $\sigma_x, \sigma_y, \sigma_z$ represent the components of the axial stresses and $\tau_{xy}, \tau_{xz}, \tau_{yz}$ represent the tangential shear stresses, $\varepsilon_x, \varepsilon_y, \varepsilon_z$ represents the linear strains, $\gamma_{xy}, \gamma_{xz}, \gamma_{yz}$ represents the angular strains, α is the coefficient of thermal expansion, ΔT is the change in temperature, G is the shear modules, ν is Poisson's ratio and E elasticity Module [19] .

Mesh study

In order to generate a pressure field on the blade surface and obtain the temperature distribution at each point of the turbine blade, this modeling consists of three different regions: the hot fluid region surrounding the blade, the cold region inside blade which compose of air that cool the blade, and the solid blade. These areas are separated by surface interfaces that must be treated precisely, especially if the mesh is not identical (non-conformal mesh) between the different areas, as is the case with us, as it is often difficult to generate an identical mesh. In this research, the flow path mesh was generated using the software (Turbogride) and generating the blade mesh using another program (Ansys meshing) as shown in **Figure 2**, as these areas are

considered a link that connects the different areas to each other, and information is transmitted from the cells of the first area to the cells of the second area through these surfaces [22].

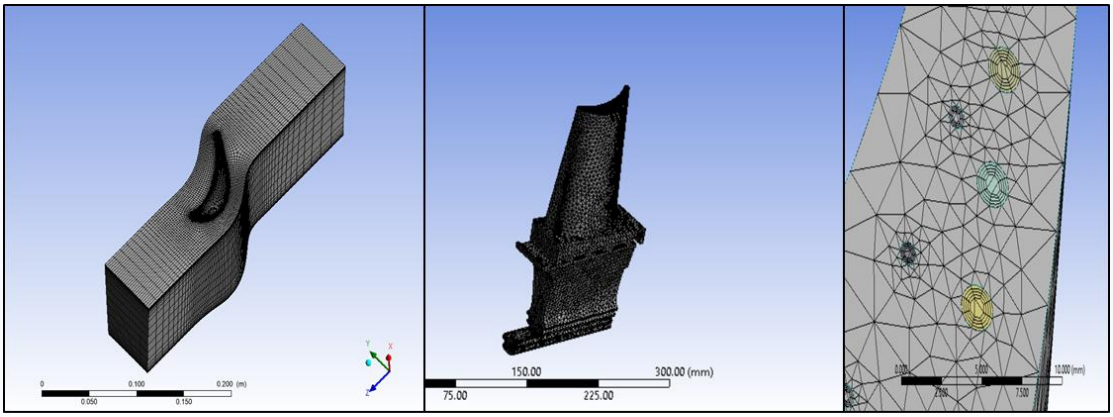

Figure 2 mesh of geometry

To ensure that the solution is valid and independent of the grid, the grid-independence of the solution was studied. For the flow field, the average temperature value on the blade surface was used along with the number of cells, while for the fatigue study, the maximum equivalent stress value was used along with the number of cells. The grid-independence study was conducted for the nickel-chromium alloy Inconel 718. The **Table 4** shows the variations in the temperature value on the blade surface with the number of cells, while the **Table** 5 shows the variations in the maximum equivalent stress value with the number of cells.

Table 4 mesh independence of flow field

Cell number	Surface blade temperature (K)
450000	1190
550000	1201
650000	1215
750000	1250
850000	1255
950000	1255
1000000	1255

Table 5 mesh independence of blade

Cell number	Max equivalent stress (MPa)
400000	723
500000	755
600000	809
700000	816
800000	816
900000	816

The characteristics of this mesh are shown in **Table** 6.

Table 6 properties of mesh

region	Cell No	Max skewness	Min skewness	Ave skewness
Flow path	860000	0.78	0.08	0.12
blade	769000	0.55	0.1	0.22

Figure 3 shows these regions with the boundary conditions placed on them, while **Table 7** shows the values of these conditions in the three regions that rotate at a constant angular speed of 3000rpm:

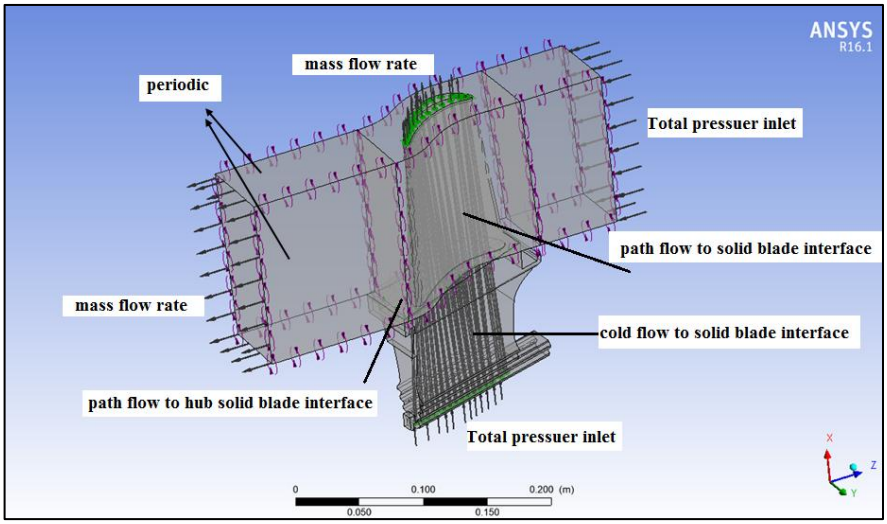

Figure 3 boundary conditions of fluid domain

Table 7 boundary conditions

region	Boundary condition	value
Hot Flow path rotate	Total Pressure inlet	11.62 bar
	Temperature inlet	1100C
	Mass flow outlet	308.2Kg/sec
	periodic	
Inner cold flow rotate	Total pressure inlet	11.62 bar
	Temperature inlet	40C
	Mass flow outlet	0.13
Solid blade rotate	-	-
mesh interface	Path flow to solid blade interface	Heat flux conservative (coupled)
	Path flow to hub solid blade interface	Heat flux conservative (coupled)
	cold flow to solid blade interface	Heat flux conservative (coupled)

Solution strategy and model validation:

The physical model of flow consists of three regions, each of which has a grid that is not identical to the grid of the other region, and information is transferred from the cells of one region to another across the surface interface. Also, solving the equations for flow and energy cannot easily converge to the required value. The solution was done using the basic solver for the CFX program, which is Pressure-Velocity coupled pseudo transient, where the solution was done first for first-order discretization, then the solution was taken as initialize solution for second-order discretization scheme, all of which are in the steady state. The physical time scale was taken to be $\Delta T = t/20$, where t represents the time of one cycle $t = 1/\omega$. it was considered that most of the flow equations for the model should converge to a value below 10^{-4}.

To ensure the validity of the solution, the isentropic efficiency of the blade was compared with the plant data. The value of this isentropic efficiency, which is 93%, we notice that it is close to the real isentropic efficiency taken from the station data, which is 89%, that is, with an error of 4.5% [1].

Fatigue analysis in the first model:

As a result of repeated and alternating loads, repetitive stresses are formed that change with time and in an alternating manner affecting the body. These oscillating and dynamic loads are called fatigue. Fatigue is considered the primary cause of more than 90% of mechanical failure of mechanical elements and equipment, as collapse of mechanical elements occurs at stresses lower than the collapse and yield stresses of the materials compared to the static state. Fatigue loads are characterized by maximum and minimum stress values like any alternating signal.

There are two approaches to fatigue analysis [8,9,12,15]:

1- Stress-life: It is based on the previous S-N diagram and is characterized by ease of analysis and is used in most designs at a high number of cycles. However, it is criticized for its lack of details and lack of accuracy. However, it is suitable for a large number of designs and will be used in this research.

2- Strain-life: It gives a more accurate and detailed analysis, but it is numerically expensive and requires the availability of information about the substance that cannot sometimes be obtained easily.

In this research we will use the stress-life approach because it is easier, less computationally expensive, and gives acceptable results.

Results and discussion:

External flow field

In order to study and see the interaction between flow field and fatigue resistance, we will show the details related to the blade made of Inconel 718 alloy and then arrange the results related to other materials as columns and final results because the flow field and stress distribution do not differ between the other materials, but the values of the studied variables differ. The **Figure 4** shows the distribution of pressure and temperatures on the surface of the main blade without cooling. We notice that the maximum temperatures are formed at the leading edge and the tail edge. We also notice a high distribution of temperatures on the belly of the blade due to the energy dissipated from the flow as a result of the vortex. The resulting energy is converted into waste heat, causing the temperature to rise at the belly of the blade, as is clear from the velocity contours in the **Figure 5**.

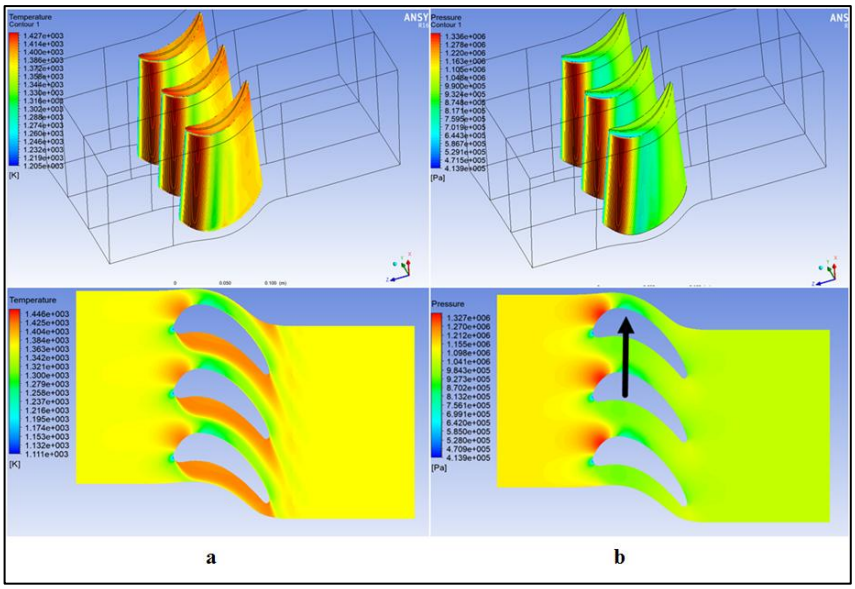

Figure 4 pressure contours for Inconel 718

By observing the relative velocity values, we notice that the stopping point occurs when the velocity values are zero, and it appears clearly in **Figure** (4-a). At this point, the pressure reaches

the greatest value (Figure 4-b), and this corresponds to the highest temperature (**Figure** 4-a), as we note. From **Figure** 5, vortexes are formed at the belly of the blade, as these vortices consume the total flow energy and dissipate this energy in the form of heat, which leads to an increase in temperature at the belly of the blade, and this is also clear from the **Figure** 5. As for the back of the blade, the flow accelerates, so its speed increases and Pressure decreases causes a decrease in temperature on the back of the blade, as shown in the previous Figures.

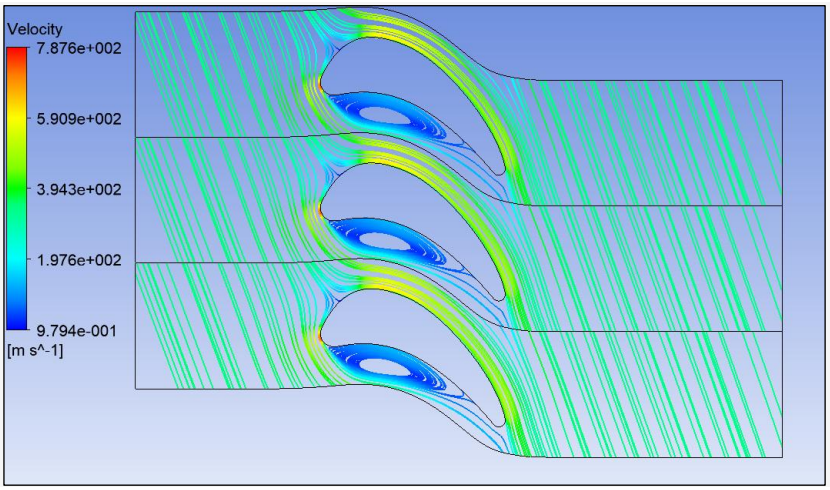

Figure 5 relative velocity values for Inconel 718

When the blade is cooled with air, the temperature distribution on the surface of the blade becomes as shown in the **Figure** 6.

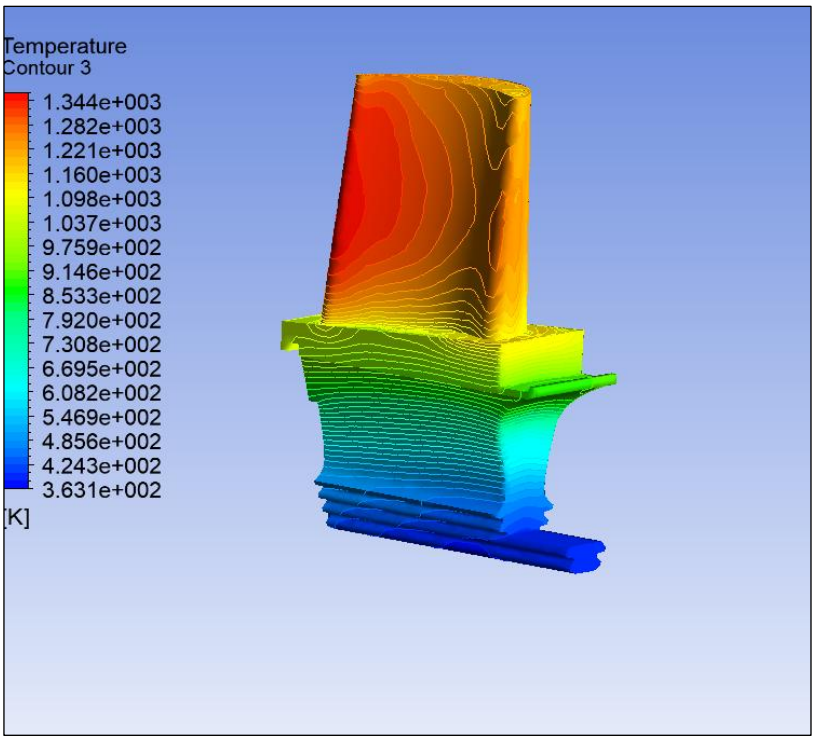

Figure 6 Temperature contours for Inconel 718

We notice a decrease in the maximum temperature values, but the temperature at the front of the blade is still high, and we notice that the average temperature on the surface of the blade decreased from 1394.28 K to 1256.95 K, i.e., by 9.85%. By analyzing the previous flow field and calculating the pressure distribution on the base of the blade and its external and internal surfaces, and by knowing the temperature distribution at each point of the blade, one way FSI coupling can be performed between Ansys CFX and Mechanical static structure to calculate the distribution of stresses and deformations occurring and perform a fatigue analysis as a result of

changing loads on the blade, where We consider every change in steady state to be a cycle of change in the loads applied to the blade. Regarding the distribution of stresses, we notice that the maximum value of the equivalent stress occurs at the blade fixation points. We will notice for other cooling paths that the location of the maximum stress changes, and we will discuss that later. We note that the value of the maximum stress is 816 MPa, which is less than the values of the yield stress, and this indicates that the blade will bear these stresses without failure to be happened, and this is shown in **Figure 7**.

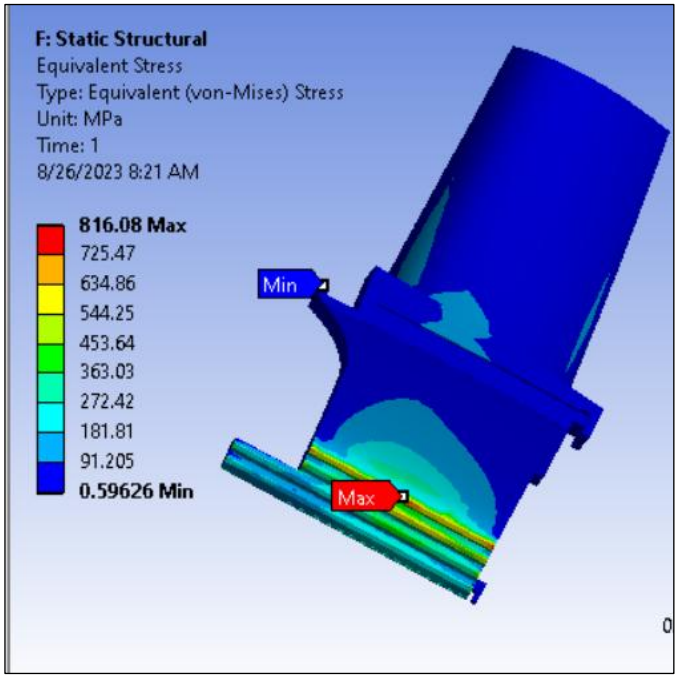

Figure 7 Equivalent stress for Inconel 718

Fatigue analysis

When analyzing stress statically, the calculated stress value at each point is taken as the amplitude of a completely reflected load (which can be changed in the program) and compared to the S-N diagram. Regarding the phenomenon of fatigue, the **Figure** 8 shows the life diagram of the blade, which means the number of cycles at which the material can collapse. The cycle here does not mean the rotation of the blade, but rather the number of times the load changes from tension to pressure, and this happens during the process of taking off, extinguishing, and moving from one state to another. From **Figure** 8, we notice that the point where the maximum stress value is the same value that can withstand a smaller number of cycles, as the life of this point, as shown in the **Figure** (8-A), does not exceed 34,000 cycles.

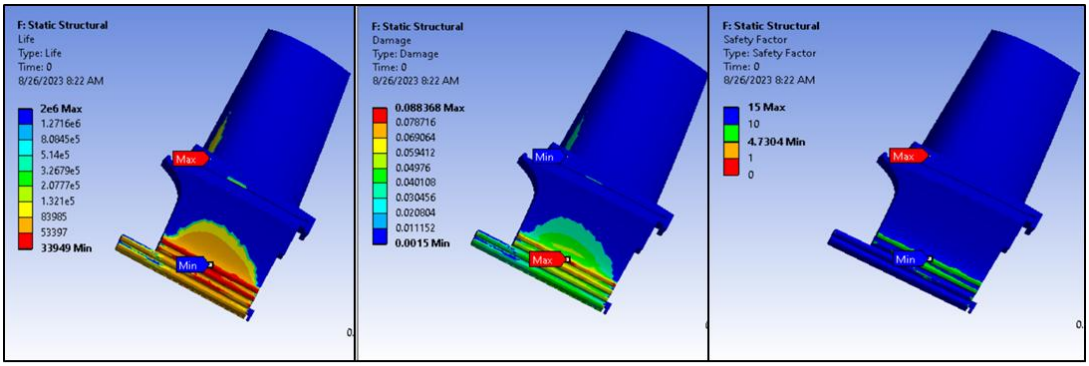

A-Life B-Damage C-Safety factor

Figure 8 fatigue analysis tools for Inconel 718

Figure (8-B) and **Figure** (8-C) show the so-called damage and safety factor. As long as the damage is less than one and the safety factor is greater than one, there is no collapse of the blade due to fatigue loads. We note that the greatest damage occurs at the lowest life point and the lowest safety factor occurs at the same point, and this occurs at the point at which the equivalent stress value is greatest. The maximum damage value is 0.088 and the minimum safety factor is.

The **Figure** 9 shows the change in the value of the maximum equivalent stress for the three materials:

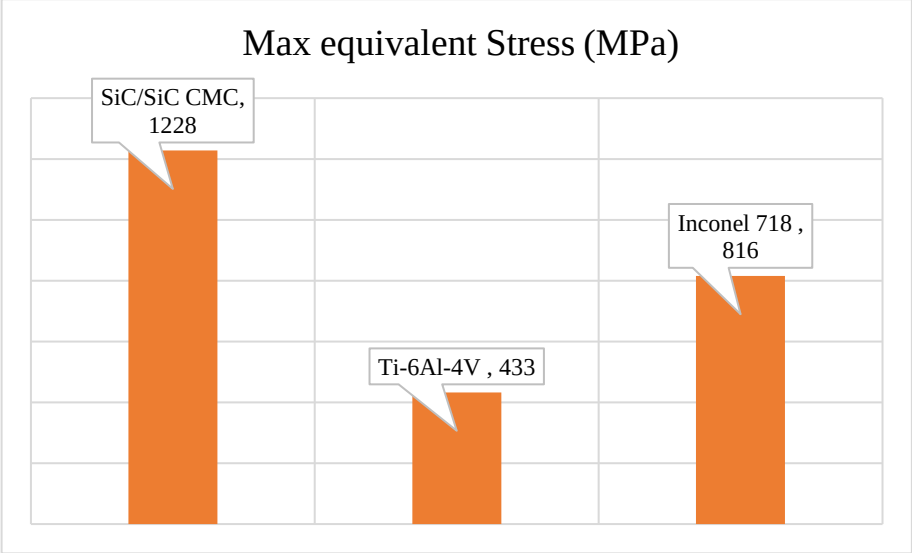

Figure 9 Maximum equivalent Stress

Numerical results showed that the maximum equivalent stress value for Inconel 718 was 816 MPa, while it decreased to 433 MPa for Ti-6Al-4V, a relative decrease of approximately 46.9%. This decrease is attributed to the softer nature of the titanium alloy, with a Young's modulus of 110 GPa, allowing it to distribute loads more uniformly and avoid stress concentration. In contrast, the equivalent stress value for the SiC/SiC composite material increased to 1228 MPa due to its higher Young's modulus, representing a 50.5% increase compared to Inconel 718 and a 183.6% increase compared to Ti-6Al-4V. This indicates that ceramic materials, despite their high hardness, are more susceptible to stress concentration and thus more susceptible to sudden collapse if they exceed the brittle fracture limits, especially if the applied loads are tensile. They will inevitably collapse, as the tensile strength of the ceramic material is around 300 MPa, but it will withstand compressive loads, as the peak compressive strength in these ceramic materials reaches 1350 MPa.

The **Figure** 10 shows the minimum life cycle value.

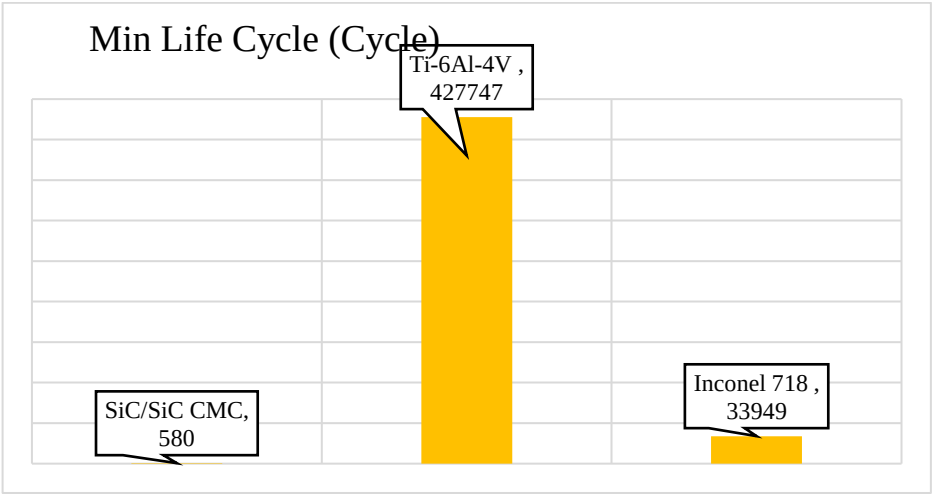

Figure 10minimum life cycle

Numerical simulation results demonstrated a decisive influence of material type on the structural performance of the blade under flow-induced loads. While the minimum fatigue life value for Inconel 718 was approximately 33,949 cycles, Ti-6Al-4V showed a significant improvement in performance, increasing its fatigue life to approximately 427,747 cycles, an increase of 1159.3%. This improvement is attributed to its ductile properties and lower Young's modulus, which allow for better stress distribution and prevents stress concentration. In contrast, the fatigue life of SiC/SiC composite materials decreased to only 584 cycles, 98.3% lower than that of Inconel 718, due to exposure to high tensile stresses that exceed the tensile strength of the brittle material. This reflects its limited use in environments with high cyclic mechanical loads, despite its high ability to withstand high temperatures.

Cumulative damage calculations using numerical modeling, as shown in the **Figure** 11, show that Ti-6Al-4V achieves a very low damage (≈ 0.007) compared to Inconel 718 (0.088), indicating a superior ability to withstand repeated loads for long periods without failure. For the SiC/SiC ceramic material, the cumulative damage exceeded the critical value (D > 1) to reach 5.12, reflecting an expected failure very early in the service life due to the material being exposed to stresses above its tensile strength in a cyclic loading environment.

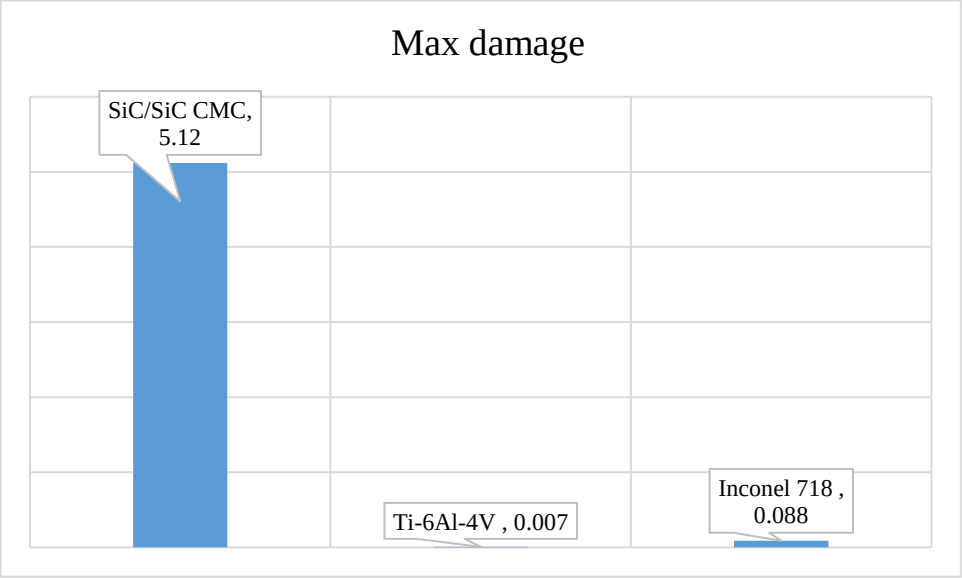

Figure 11maximum damage

Numerical modeling results showed a clear variation in the minimum fatigue safety factor between the three materials, as shown in the **Figure 12**. Inconel 718 alloy showed a very high safety factor (4.73), reflecting a good match between its mechanical properties and flow and stress conditions. In contrast, Ti-6Al-4V alloy recorded a low safety factor (1.18), indicating that it is close to the safe performance limits and requires careful design tuning to avoid fatigue failure. The SiC/SiC ceramic material recorded a very low safety factor (0.285), indicating it would be weak to cyclic loads in the current flow environment. The brittle nature was the issue, as well as a low tensile fatigue limit, and the use of this material would not be possible for a safety factor<1, unless the design was changed or mechanical protection was added to allow for usage in some environments.

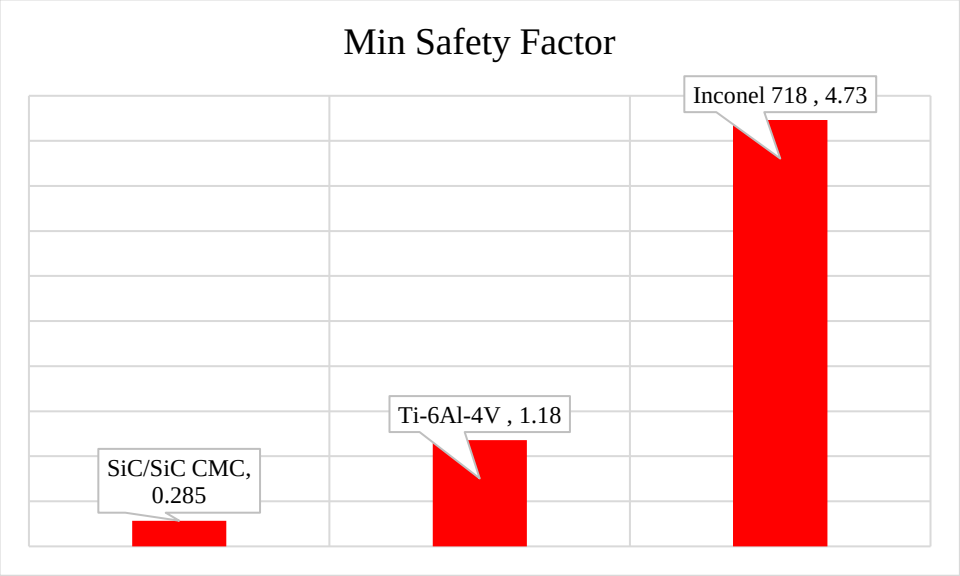

Figure 12 Minimum safety factor

This may be summarized as follows:

Inconel 718 is a strong alloy that provides a nice balance of stiffness and ductility and is still useful for stress reduction and stress dissipation, although not to the degree of other materials. It is specifically designed to handle cyclic and thermal stresses, in serious applications like gas turbine blades under horrible situations. It also boasts an extremely high fatigue limit that is above 1200 MPa under optimum conditions. It also exhibits ductility that can potentially allow the re-distribution of loads and not concentrate them at weak locations, and it has a high safety factor which implies it is very capable of handling a load without premature failure .

The Ti-6AI-4V Titanium alloy is not as stiff as an Inconel, however, it provides flexibly absorbed stresses without the concentration of stress at critical locations.. A 46.9% reduction in equivalent stress yields an 11-fold gain in fatigue life, indicating a strong capacity to endure cyclic loads. Its ductile qualities allow it to absorb rather than concentrate stresses, but its fatigue limit is lower, at roughly 510 MPa. As a result, its safety factor is close to one, making it appropriate for use in low- to medium-stress applications.

SIC/SIC CMC is a naturally fragile substance. Despite its great thermal capacity and hardness, its main disadvantage is that it cannot tolerate cyclic tensile stresses. It has a low tensile fatigue limit (300-400 MPa) and a high Young's modulus, making it resistant to stretching and deformation. When this combination is subjected to an equivalent stress larger than its bearing capacity, microcracks begin to form, and there is insufficient elasticity to prevent breakage. Its safety factor is less than one, indicating that the material will certainly fail under applied loads. This does not imply that it is "evil," only that it is unsuitable for this sort of repeated mechanical use.

Based on numerical and mechanical analysis, Inconel 718 is the ideal material for gas turbine blades among the materials investigated, owing to its high fatigue resistance, high safety factor, and ability to sustain high temperatures without structural collapse. Although Ti-6Al-4V provides sufficient performance, it works near its safety limits, necessitating prudence in usage. Despite their better heat conductivity, SiC/SiC composites are very brittle and cannot tolerate cyclic pressures, rendering them unsuitable for this sort of application without significant design changes or additional protective mechanisms.

Conclusion

A comprehensive numerical investigation of the influence of flow field on the wear resistance of gas turbine blades using three different materials yielded the following results:

Ti-6Al-4V had a 46.9% lower equivalent stress value than Inconel 718, resulting in an 1159.3% increase in service life. SiC/SiC had a 50.5% higher equivalent stress value than Inconel, but fatigue life was reduced by 98.3%. Cumulative damage exceeded five times the allowed limit, suggesting premature failure. The minimal safety fatigue factor was 4.73 for Inconel 718, 1.18 for Ti-6Al-4V, and 0.285 for SiC/SiC, demonstrating Inconel's better performance under harsh working circumstances. These findings show that Inconel 718 is the best choice for gas turbine applications because to its outstanding combination of heat and fatigue resistance, whereas Ti-6Al-4V may be employed in medium-strength applications, and SiC/SiC requires unique design methods to compensate for its high brittleness under cyclic loads.

References

1. Boyce MP. Gas turbine engineering handbook. 3rd ed. Amsterdam: Elsevier; 2006.
2. Song YJ, Li T, Zhang D, et al. Review of gas turbine blade internal cooling with ribs. Therm Turbine 2011;40(4):235–244 [Chinese].
3. Patil PS, Borse SL. Recent studies in internal cooling of gas turbine blade: A review. Int J Appl Eng Res 2018;13(9):7131–41.
4. Yin Z, Fang XJ. Multi-objective optimization of film-cooled turbine with source term method. J Propuls Technol 2013;34 (10):1339–44[Chinese].
5. Yu K, Yang X, Yue Z. Aerodynamic and heat transfer design optimization of internally cooling turbine blade based different surrogate models. Struct Multidiscip Optim 2011;44(1):75–83.
6. Nowak G, Wro´ blewski W. Thermo mechanical optimization of cooled turbine vane. Proceedings of ASME turbo expo 2007: Power for land, sea, and air. New York: ASME; 2007.
7. Li, P., Choi, J. H., Zhang, D., Zhang, S., & Zhang, Y. (2025). Reinforced symbolic learning with logical constraints for predicting turbine blade fatigue life. *Aerospace Science and Technology*, *158*, 109888.
8. Sun, D., & Wan, Z. (2024). Experimental study and life prediction for aero-engine turbine blade considering creep-fatigue interaction effect. *Engineering Fracture Mechanics*, *310*, 110507.
9. Zalapa Garibay, M. A., Guillén Anaya, L. G., Clemente, C., Rodríguez Ramírez, J. A., & García Castrejón, J. C. (2023). Corrosion Fatigue Analysis in Power Steam Turbine Blade. *Instituto de Ingeniería y Tecnología*.
10. Li, M., Gao, J., & Zhou, J. (2025). A Combined High and Low Cycle Fatigue Life Prediction Model for Wind Turbine Blades. *Applied Sciences*, *15*(3), 1173.
11. Shah, I., Khan, A., Ali, M., Shahab, S., Aziz, S., Noon, M. A. A., & Tipu, J. A. K. (2023). Numerical and experimental analysis of horizontal-axis wind turbine blade fatigue life. *Materials*, *16*(13), 4804.
12. Gonabadi, H., Oila, A., Yadav, A., & Bull, S. (2022). Fatigue life prediction of composite tidal turbine blades. *Ocean Engineering*, *260*, 111903.
13. Patel, D., & Nair, K. Comparative Study of Fatigue Analysis of Horizontal Axis Wind Turbine Blade Materials.
14. Dhimole, V. K., Yu, G., & Cho, C. (2024). Failure assessment of braided ceramic matrix composite dovetail turbine blade under thermo-mechanical load. *Journal of the Korean Ceramic Society*, *61*(6), 1278-1290.
15. Kim, K., & Lee, Y. S. (2014). Modal characteristics and fatigue strength of compressor blades. *Journal of Mechanical Science and Technology*, *28*(4), 1421-1429.

16. Sanchez-Botello, X., de la Torre, A., Roig, R., Jou, E., de la Torre, O., Ayneto, J., & Escaler, X. (2023). Experimental and numerical study on the detection of fatigue failure in hydraulic turbines. *Journal of Mechanical Science and Technology*, *37*(10), 4949-4955.
17. A, P. Fraas, summary of research and development effort on air and water cooling of gas turbine blades, a. P. Fraas, oak ridge, tennessee 37830, date published - march 1980.
18. K. Sagae, N. Kizuka, K. Kawaike, S. Anzai, S. Marushima and T. Ikeguchi, Power Industrial Systems,R&D Division,R&D for 1700C-class Turbine Closed Loop Cooled Blades,Hitachi Ltd., Ibaraki, 312-0034, Japan,1999.
19. Xing-dan Zhu, Jing-zhou Zhang, Xiao-ming Tan, Numerical assessment of round-to-slot film cooling performances on a turbine blade under engine representative conditions, College of Energy and Power Engineering, Jiangsu Province Key Laboratory of Aerospace Power System, Nanjing University of Aeronautics and Astronautics, 2019, China.
20. Suraj Gavali1, Dipali. S. Garad2, Prof. Jayawant N. Yadav3, Review of Cooling of Gas Turbine Blades, International Journal of Applied A.Hoffmann, K. (2000). Computational Fluid Dynamics. USA: Engineering Education System.
21. ANSYS CFX documentation: Theory guide, 2016. (n.d.).
22. ANSYS CFX documentation: User guide, 2016. (n.d.).
23. Çengel, y. A. (2014). Fluid mechanics: fundamentals and applications, third edition. New york: mcgraw-hill.
24. Thermal properties of cast nickel based super alloy Article in Archives of Materials Science and Engineering · July 2010-Source: DOAJ**.**